CELL VIABILITY WITHIN ORAL BIOFILMS

C. K. Hope and M. Wilson

Microbiology Unit,

Eastman Dental Institute for Oral Health Care Sciences,

University College London,

256 Gray's Inn Road,

WC1X 8LD

Abstract

Bacteria are not distributed homogenously throughout an oral biofilm. This is primarily due to regions of differing environmental conditions, themselves a manifestation of nutrient, gaseous and ionic concentration gradients within the biofilm. Confocal laser scanning microscopy in conjunction with fluorescent staining techniques and image analysis can both visualise and quantify the distribution of viable and nonviable bacteria within the three-dimensional volume of the biofilm.

Introduction

Dental plaque is a biofilm that forms on the tooth / saliva interface in the oral cavity. The primary component of *any* biofilm is an extracellular matrix which constitutes most of the volume occupied by the biofilm. The matrix is primarily composed of water and aqueous solutes, with the balance of the dry weight consisting of exopolysaccharides, proteins, salts and cellular material. Bacterial cells are suspended within this matrix. A biofilm is not, however, a homogenous structure (Wimpenny *et al*., 2000) and as such the bacteria are not distributed evenly throughout.

On the scale of the constituent microbial population, an oral biofilm cannot be considered to be a two dimensional layer, but rather a three-dimensional ecosystem containing within it a variety of different microenvironments. There is a constant flux in the availability of oxygen and nutrients in the biofilm alongside more permanent depth-related gradients. Biofilms contain structures such as water channels, voids and have surface protrusions often termed "towers" or "stacks" (Cowan *et al*., 2000). These structures are assumed to develop in order to maximise the surface area of the biofilm in contact with the external environment.

The constant-depth film fermenter (CDFF) (University of Wales, Cardiff) (Peters *et al*., 1988) is capable of producing a steady-state oral biofilm community (Kinniment *et al*., 1996) and is considered to be more representative of the phase interface conditions occurring *in vivo* than submerged chemostat based systems (Wimpenny, 1999). The basis of the CDFF is a rotating turntable which holds recessed discs of an appropriate

substratum (e.g. tooth enamel, hydroxyapatite). Nutrient medium is dripped onto the turntable and spread over the discs by the action of scraper blades. This action also serves to remove excess cellular material growing out of the recess, maintaining the biofilms at a constant depth.

The following environmental conditions and operating parameters are user-definable during operation of the CDFF:

1. Temperature
2. Bacterial composition (i.e. choice of inoculum, enrichment nutrient regimes)
3. Oxygen tension
4. Ionic composition
5. Biofilm depth
6. Nutrients
7. "Saliva" flow rate
8. Shear forces (a function of flow rate and angular velocity of the turntable)

By adjusting these parameters to model the growth conditions found within dental plaques, the CDFF has been shown to be capable of producing oral biofilms which are comparable to their *in vivo* counterparts on the basis of the following criteria:

1. Microbiological composition (Kinniment *et al.*, 1996)
2. Succession of bacteria from microcosm inoculum (well established)
3. Formation of inter species co-aggregation structures such as corn-cobs and chains (well established)

4. Response to nutrient stress (Pratten *et al*., 2000)
5. pH profile response to sucrose (Vroom *et al*., 1999)
6. Population response to sucrose (Pratten *et al*., 1999)
7. Transfer of mobile genetic elements between bacteria (Roberts *et al*., 1999)
8. Spatial distribution of cell vitality (Auschill *et al*., 2001;Hope *et al*., 2002)
9. Surface topography of the biofilm (Wood *et al*., 2000) (Hope *et al*., 2003)

These features of CDFF-grown oral biofilms allow reproducible, direct comparisons and extrapolations to be made between these *in vitro* biofilms and their *in vivo* dental plaque counterparts.

Confocal laser scanning microscopy (CLSM) involves taking a series of thin optical sections at different depths through a sample. This is attained by employing a pinhole aperture to block out-of-focus light resulting in an image with a very narrow depth of field (~1 μm). A series of optical sections ("slices") are typically taken at different depths into the sample and subsequently combined by computer to form a "stack". The term "image stack" will be used herein to distinguish between a series of optical sections and biofilm surface features ("biofilm stacks"). CLSM is normally used in conjunction with fluorescent dyes, which stain and highlight specific regions within the sample. The *Bac*Light™ (Molecular Probes, OR, USA) LIVE/DEAD stain system is used to differentiate between viable and nonviable bacteria on the basis of membrane integrity. Bacteria with intact cell membranes exhibit green fluorescence upon excitation, whilst bacteria with damaged membranes fluoresce red. CLSM detector systems can be set to

distinguish between these two fluorophores and record each channel as a separate image stack.

This chapter discusses the methods available to visualise the distribution of cell viability, as detected by vital staining in conjunction with CLSM of CDFF-grown oral biofilms.

Materials and Methods

Growth of Oral Biofilms in the CDFF

Preparation of the Inoculum

Saliva was collected from 20 healthy individuals, aged 20-40 years, a mixture of smokers and non-smokers. 5ml of phosphate buffered saline was added to each of these before being pooled. Glycerol (BDH Cehmicals, Poole, UK) was then added to the pool to act as a cryoprotectant giving a final concentration of 15% v/v. The saliva pool was then split into 2ml aliquots before storage at -80ºC.

Operation of the CDFF

These procedures have been described in detail previously (Wilson, 1999). In brief, the CDFF was loaded with 5mm hydroxyapatite discs recessed to a depth of 200µm, sterilised and then incubated at 37ºC. One litre of a complex, mucin-containing artificial saliva (AS) (Pratten *et al*., 1998) was inoculated with a 2ml aliquot of the saliva pool. This was incubated at 37ºC and pumped into the CDFF, at a rate of 0.7ml min^{-1}, the mean salivary flow rate in man (Guyton and Hall 1997;Lamb, Ingram *et al.* 1991). Sterile AS was pumped concurrently into the CDFF, also at a rate of 0.7ml min^{-1}. The CDFF was exposed to the atmosphere via a 0.2µm filter. The movement of air (and therefore oxygen) into the interior of the CDFF was by diffusion only. Sample pans, each containing five HA discs and their incumbent biofilms, were removed from the CDFF after a minimum of eight days growth.

Confocal Laser Scanning Microscopy of Oral Biofilms

Sample Preparation

After extrication of a sample pan from the CDFF, a single biofilm-covered HA disc was gently rinsed in PBS to remove excess AS and bacteria present in the liquid phase above the biofilm proper. The disc was then placed onto a drop (10µl) of PBS in a sterile bijou. The drop of PBS was included to humidify the atmosphere within the bijou and also served to hold the disc in place by surface tension during transport to the confocal microscope.

Confocal Laser Scanning Microscopy

A liquid viewing medium comprising of 8ml PBS with 2µl each of components A and B (*Bac*Light LIVE/DEAD stain) was chilled to 4ºC and protected from light to prevent degradation of the dyes. A number of HA discs (typically four) were placed into a small cell-culture dish (total capacity of approximately 15ml), with the biofilm facing upwards. The liquid viewing medium was then carefully poured into the dish and allowed to cover the biofilms.

The biofilms were then examined by a Leica DMLFS (Leica, Milton Keynes, Northamptoshire, UK) fixed stage microscope with a Leica TCS SP (and later SP2) confocal laser scan-head. Water-dipping objective lenses (Leica) were used to view the biofilms whilst they were still immersed in the liquid viewing medium. The photomultiplier (PMT) settings were set to maximise the contrast range of the images for both the LIVE and DEAD fluorescent excitation channels which were either scanned in

combination or sequentially, depending upon the degree of crosstalk (signal overlap) between the two fluorophores. The *z*-axis step size was typically set at 1 - 4µm intervals depending upon the thickness of the image stack. Images were captured in 8-bits (pixel brightness range) at a resolution of 512 x 512 pixels using Leica TCS NT software. The images were then archived onto optical discs for later analysis. Each scan produced two image stacks, one for each of the fluorescent dye excitation channels

Image Analysis

These techniques were utilised to manipulate a range of image parameters such as brightness, filtering, and threshold levels within user-specified values but, more importantly, to return numerical values to describe images. These functions were employed upon individual slices or the entire image stack, based upon voxel (a three-dimensional pixel) brightness. The techniques described below were carried out using a Java™ (Sun Microsystems, CA, USA) based image analysis software package, ImageJ (Rasband, 2003).

Viability Profiling

ImageJ's "plot z-axis profile" function was employed upon the whole image stacks of the two different fluorescence channels, yielding values for mean pixel brightness (0 - 255) against slice (optical section) number. These data were then exported to a spreadsheet package, Excel™ (Microscoft Corp, WA, USA) where the pixel values were normalised (i.e. the maximum mean pixel brightness for each channel was assigned a value of 1 unit). The following plots were then constructed (Hope *et al.*, 2002):

1. Normalised fluorescence value for LIVE and DEAD (units) versus depth (µm)
2. LIVE minus DEAD normalised fluorescence value (units) versus depth (µm)

Viability Mapping

This process was used to elucidate the distribution of vital staining in the *x*-*y* plane for a number of adjacent optical sections. Image analysis techniques were also engaged to measure the size of features revealed by the differences in vital staining. The most interesting, measurable feature observed in biofilm stacks was the existence of an outer layer of viable bacteria surrounding a nonviable inner core (Hope *et al.*, 2003). These structures were by no means ubiquitous, but possessed an easily distinguishable motif, the dimensions of which could be measured. The thickness of an outer layer of biofilm as revealed by vital staining has been termed *blanket thickness*.

Image stacks were first combined into a single RGB (red-green-blue, i.e. full colour) image stack using the ImageJ, "RGB Merge" function. The LIVE stack was assigned the green channel, the DEAD stack was assigned the blue channel whilst the red channel was unused (see discussion). The resulting RGB stacks were then examined to find (adjacent, if possible) slices exhibiting a viable outer layer. ImageJ's "freehand selection" tool was then used to draw around the boundaries of the viable and nonviable regions (figure 1), the areas (A) of these two regions were then determined by the ImageJ "measure" function and the radii (r) calculated by the equation:

$$r = \sqrt{\frac{A}{\pi}}$$

The blanket thickness in the *x*-*y* plane was the radius of the outer (LIVE/bulk medium) boundary minus the radius of the inner (LIVE/DEAD) boundary. This process was repeated for different slices / image stacks and the average blanket thickness determined.

The variation in the spatial distribution of LIVE and DEAD fluorescence was also demonstrated by a more conventional image analysis technique; ImageJ's "plot profile" command. This feature returned the pixel brightness values along a user-selected line of interest in the original LIVE and DEAD image stacks, the results of this process were then exported to Excel and plots produced. When conducted upon the original images, these plots often contained high levels of noise due to the pixelated nature of confocal micrographs. The noise was reduced before analysis by "smoothing" the original image. A reproducible method of smoothing was to pass the image through the "Gaussian blur" or "mean" filter set to between 2 and 8 pixels radius and / or by selecting a narrow-rectangular region of interest (ROI) across the image; this was effectively the average of *n* adjacent parallel lines of interest. Noise was also reduced (or more accurately ignored) post-analysis by applying 4^{th} order polynomial lines of best fit to the data in Excel.

Stack Rendering

Mathematical descriptions of images and their stacks were complemented by rendering, which allowed image stacks to be moved and viewed as three-dimensional objects by computer. Two forms of rendering were suitable for the volumisation of image stacks; surface rendering and volume rendering.

Surface Rendering

The first step in surface rendering was to produce a surface topograph using proprietary confocal microscopy software (Leica Microsystems GmbH, 2002). This produced a two-dimensional image where depth was represented by a greyscale gradient. A (virtual) surface was then constructed by computer (windows based PC) and wrapped around the topographical data.

The procedure for producing surface renderings from image stacks in ImageJ requires the VolumeJ plug-in (Abramoff *et al*., 2002), the methodology and background of this procedure are described online (Abramoff, 2003).

Volume Rendering

The underlying principle of volume rendering is that the optical sections are moved in perspective, thus creating the illusion of depth. A degree of transparency can be incorporated into the image stack, enabling one to visualise structures within the biofilm in three dimensions. However, the image stack must continue to move in order to maintain the perception of three dimensions, cessation of movement destroys the depth element. As such this process does not translate to static media such as paper.

The first step of volume rendering using ImageJ was to open the image stack files containing the two fluorescent channels. The "3D project" function was applied to both the LIVE and DEAD image stacks using the default settings with the following exceptions:

Projection method	> brightest point
Axis of rotation	> y-axis
Slice interval	> set to the z-axis step size
Initial angle	> -20º
Total rotation	> 40º (i.e. double the initial angle)
Rotation increment	> 2º

" interpolate when slice spacing > 1.0" enabled

The resulting projections were then combined as a single RGB image stack with the "RGB color merge" function. The LIVE channel was assigned green; the DEAD channel blue. A considerable amount of pixel brightness information was lost by the volume rendering process and the combined RGB images were often saturated by a single colour channel. As such it was often necessary to adjust the brightness and contrast of the two volume renderings before they were combined or adjust copies of the original image stacks.

Results

Figure 1 shows a single optical section through a CDFF-grown oral biofilm exhibiting the structural motif of an outer layer of viable bacteria surrounding a nonviable inner region. This figure is shown as a negative for clarity. The ROI was 20 pixels wide and the image had passed through ImageJ's "mean" filter set at a radius of 5 pixels. The plot-profile across the region of interest presents a mathematical description of the blanket thickness phenomenon (figure 2).

The viability profiles shown in figures 3a - 3c are examples of the different forms we have so far observed in oral biofilms. Figure 3a shows the typical pattern of the progression from LIVE to DEAD fluorescence as the optical sections penetrate deeper into the biofilm, whereas the profile shown in figure 3b yields the opposite sequence. Figure 3c shows an example of a less well defined viability profile.

Figure 4 is an example of a surface topograph constructed using Leica LCS Lite. The image is depth-coded; white representing the top of the image stack, moving down to black through a distance of 50 µm. The corresponding surface rendering from this topographical data is shown in figure 5.

Viability mapping techniques have shown the outer layer of viable bacteria in an interproximal plaque model grown in a CDFF to have a mean thickness of approximately 35µm in the *x-y* plane (Hope *et al.*, 2003).

Discussion

LIVE/DEAD staining is an effective tool to differentiate between viable and nonviable bacteria. When used in conjunction with CLSM, the heterogeneity of the spatial distribution of viable and nonviable bacteria can be quantified.

It is widely reported that the fidelity of the LIVE/DEAD stain is not 100% accurate in terms of differentiating between those cells which are viable and those which are nonviable. For example, small numbers of DEAD fluorescing bacteria have been observed to have an active metabolism and be capable of cell division. We do however consider the LIVE/DEAD stain system to be suitable for elucidating trends in viability through mixed populations of bacteria forming oral biofilms. It is doubtful that any of the structural motifs described here are artefacts of the differential penetration of the LIVE/DEAD stains into the matrix of biofilm. The two components of the LIVE/DEAD stains, SYTO9™ and propidium iodide have similar molecular weights, both posses a net negative charge and the gross shape of the molecules (i.e. tightly folded, linear or branched) can be assumed to be not too dissimilar (proprietary information). During the confocal microscopic examinations described here, the dyes were allowed to develop for approximately fifteen minutes before the first scan was taken. Subsequent scans were taken after the biofilm had been immersed in the liquid viewing medium, containing the LIVE/DEAD stain, for up to 2 hours. Photobleaching (van den Engh *et al*., 1992) of the LIVE/DEAD stain components was not an issue in this system since there was a constant flux of the dyes into the biofilm from the liquid viewing medium to replace any photobleached dye molecules.

Not all the biofilms we examined showed the marked contrast between the outer layers of viable bacteria and inner nonviable bacteria reported and measured here. The boundaries between viable and nonviable regions were often too indistinct. Automated threshold methods were unable to reproducibly differentiate the boundary between the LIVE and DEAD staining regions. Manual measurements have proved to be accurate and reproducible (Hope *et al.*, 2003).

The raw pixel brightness information for the LIVE and DEAD stains cannot be directly compared since the dyes have different excitation / emission wavelengths and are detected separately. However, the spatial distribution of viable and nonviable staining bacteria, as detected by the two different fluorophores, can be compared with a degree of certainty. The LIVE-green, DEAD-blue colour scheme is considered to be easier to differentiate than the original red/green emission of the dyes. The green/blue format also allows colour-blind individuals (~5% of the population) to differentiate the LIVE and DEAD staining regions.

We can only hypothesise as to why the inner regions of the CDFF grown biofilms appear to contain a higher proportion of nonviable bacteria than the biofilm in contact with the bulk medium. The deeper layers of the biofilm will have a lower availability of oxygen, less access to primary nutrients and a higher concentration of secondary metabolites than the outer layers (Xu *et al.*, 1998). These conditions ought to provide a separate, discrete ecological niche that should normally be filled by the anaerobic cohort of the bacterial

population found in similar interproximal CDFF biofilms such as *Veillonella* spp. (Hope and Wilson, 2003). A possible explanation for the lower proportion of viable bacteria within the biofilm is that they become temporally dislocated from their optimal growth conditions. As the biofilm develops over time, primary colonising aerobic bacteria that were originally in contact with the bulk medium become overgrown by the developing biofilm. The concentration of secondary metabolites will also exacerbate this. These ensuing changes in the proximal environment eventually conspire to kill the bacteria (see figure 6).

Viability profiles support the results of a previous study (Pratten *et al.*, 1998) which reported upon the distribution of bacteria in terms of viability and speciation through a multi-species oral biofilm. These CDFF-grown oral biofilms were examined by cryosectioning and the proportion of LIVE/DEAD staining bacteria recorded along with numbers of viable bacteria from each of the different incumbent species. They too found that the deeper layers of the biofilm contained more nonviable bacteria than the surface layers. The results regarding the distribution of different species through the depth of the biofilm were however considered "surprising". The obligate anaerobe *Veillonella dispar* was found to be distributed evenly through the depth of the biofilms, although it was quite reasonably assumed that it should be found in greater number in the deeper, anaerobic layers of the biofilm. Conversely, the obligate aerobe *Neisseria subflava* was distributed as expected, being the predominant organism in the upper layers, it's numbers reducing with depth into the biofilm. These results show that the flux of nutrients and oxygen with depth constitute only some of the factors which contribute to the

heterogeneous distribution of bacteria in biofilms. The pH profile observed through the depth of an oral biofilm (Vroom *et al.*, 1999) and the accumulation of secondary metabolites are no doubt other significant, contributory factors behind the spatial distribution of bacterial viability in biofilm.

In summary, a variety of different viability distributions in oral biofilms have been observed by CLSM in our own and other studies:

1. Viable bacteria surrounding an inner core (or lower layers) of nonviable bacteria (Auschill *et al.*, 2001;Hope *et al.*, 2002;Hope *et al.*, 2003;Netuschil *et al.*, 1998)
2. A background of viable bacteria with small clusters (individual cells) of nonviable bacteria distributed within the *x-y* plane of the biofilm (Hope *et al.*, 2003)
3. A background of nonviable bacteria with clusters of viable bacteria distributed within the *x-y* plane of the biofilm (Auschill *et al.*, 2001)
4. Nonviable bacteria surrounding an inner core of viable bacteria (E. Zaura-Arite, unpublished data; C. Hope unpublished data; figure 3b - DEAD to LIVE viability profile)
5. Viable bacteria surrounding a void (or region containing low numbers of weakly fluorescing nonviable bacteria) (Auschill *et al.*, 2001;Hope *et al.*, 2002)

The distribution of bacterial vitality is far more complicated than that predicted by current models of concentration gradients into the depth of the biofilm. The image analysis techniques described herein, viability profiling and viability mapping, produce mathematical descriptions of the distribution of viable and nonviable bacteria in an oral

biofilm. These techniques can be supplemented with rendering processes to allow the visualisation of these trends. Surface renderings can produce useful data regarding the "physical" properties of the biofilm topography; whereas volume renderings are preferred for visualising biofilms in three-dimensions. These measurements and imaging techniques allow us to better understand the mechanisms behind the spatial distribution of bacterial vitality in biofilms and may ultimately be used to quantify the effects of antimicrobial compounds upon oral biofilm (O'Neill *et al*., 2002).

Acknowledgements

Funding for this work was provided by Philips Oral Healthcare.

REFERENCES

Abramoff, M. D. (2003). VolumeJ version 1.61. (Freeware) http://bij.isi.uu.nl/vr.htm

Abramoff, M.D. and Viergever, M.A. (2002). Computation and visualization of three-dimensional soft tissue motion in the orbit. *IEEE Trans Med Imaging* **21**, 296-304.

Auschill, T.M., Arweiler, N.B., Netuschil, L., Brecx, M., Reich, E., Sculean, A. & Artweiler, N.B. (2001). Spatial distribution of vital and dead microorganisms in dental biofilms. *Arch Oral Biol* **46**, 471-476.

Cowan, S.E., Gilbert, E., Liepmann, D. & Keasling, J.D. (2000). Commensal interactions in a dual-species biofilm exposed to mixed organic compounds. *Appl Environ Microbiol* **66**, 4481-4485.

Guyton, A.C. and Hall, J.E. (1997). Secretary functions of the alimentary tract. In *Human physiology and mechanisms of disease*, pp. 524-536. Edited by Schmitt, W. Philadelphia: Saunders.

Hope, C.K., Clements, D. & Wilson, M. (2002). Determining the spatial distribution of viable and nonviable bacteria in hydrated microcosm dental plaques by viability profiling. *J Appl Microbiol* **93**, 448-455.

Hope, C.K. & Wilson, M. (2003). Effects Of dynamic fluid activity from an electric toothbrush on i*n vitro* oral biofilms. *J.Clin.Periodontol.* (In press).

Hope, C.K. and Wilson, M. (2003). Measuring the thickness of an outer layer of viable bacteria in an oral biofilm by viability mapping. *Journal of Microbiological Methods* **54**, 403-410.

Kinniment, S.L., Wimpenny, J.W., Adams, D. & Marsh, P.D. (1996). Development of a steady-state oral microbial biofilm community using the constant-depth film fermenter. *Microbiology* **142**, 631-638.

Lamb, J.F., Ingram, C.G., Johnston, I.A. & Pitman R.M. (1991). Gastrointestinal system and nutrition. In *Essentials of physiology*, pp. 91-115. Edited by Oxford: Blackwell Scientific Publications.

Leica Microsystems GmbH. (2002). Leica Confocal Software Lite version 2 Build 0871. (Available via file transfer protocol) Mannhiem, Germany ftp://ftp.llt.de/pub/softlib/LCSLite/

Netuschil, L., Reich, E., Unteregger, G., Sculean, A. & Brecx, M. (1998). A pilot study of confocal laser scanning microscopy for the assessment of undisturbed dental plaque vitality and topography. *Arch Oral Biol* **43**, 277-285.

O'Neill, J.F., Hope, C.K. & Wilson, M. (2002). Oral bacteria in multi-species biofilms can be killed by red light in the presence of toluidine blue. *Lasers Surg Med* **31**, 86-90.

Peters, A.C. and Wimpenny, J.W. (1988). A constant depth laboratory film fermenter. *Biotechnology and Bioengineering* **32**, 263-270.

Pratten, J., Barnett, P. & Wilson, M. (1998). Composition and susceptibility to chlorhexidine of multispecies biofilms of oral bacteria. *Appl Environ Microbiol* **64**, 3515-3519.

Pratten, J., Bedi, R. & Wilson, M. (2000). An in vitro study of the effect of fluoridated milk on oral bacterial biofilms. *Appl Environ Microbiol* **66**, 1720-1723.

Pratten, J. and Wilson, M. (1999). Antimicrobial susceptibility and composition of microcosm dental plaques supplemented with sucrose. *Antimicrob Agents Chemother* **43**, 1595-1599.

Rasband, W. (2003). ImageJ [PC Program] version 1.29x. (Freeware) . National Institutes of Health, USA http://rsb.info.nih.gov/ij/

Roberts, A.P., Pratten, J., Wilson, M. & Mullany, P. (1999). Transfer of a conjugative transposon, Tn5397 in a model oral biofilm. *FEMS Microbiol Lett* **177**, 63-66.

van den Engh and Farmer, C. (1992). Photo-bleaching and photon saturation in flow cytometry. *Cytometry* **13**, 669-677.

Vroom, J.M., De Grauw, K.J., Gerritsen, H.C., Bradshaw, D.J., Marsh, P.D., Watson, G.K., Birmingham, J.J. & Allison, C. (1999). Depth penetration and detection of pH gradients in biofilms by two-photon excitation microscopy. *Appl Environ Microbiol* **65**, 3502-3511.

Wilson, M. (1999). Use of constant depth film fermentor in studies of biofilms of oral bacteria. *Methods Enzymol* **310:264-79.**, 264-279.

Wimpenny, J. (1999). Laboratory models of biofilm. 89-110.

Wimpenny, J., Manz, W. & Szewzyk, U. (2000). Heterogeneity in biofilms. *FEMS Microbiol Rev* **24**, 661-671.

Wood, S.R., Kirkham, J., Marsh, P.D., Shore, R.C., Nattress, B. & Robinson, C. (2000). Architecture of intact natural human plaque biofilms studied by confocal laser scanning microscopy. *J Dent Res* **79**, 21-27.

Xu, K.D., Stewart, P.S., Xia, F., Huang, C.T. & McFeters, G.A. (1998). Spatial physiological heterogeneity in Pseudomonas aeruginosa biofilm is determined by oxygen availability. *Appl Environ Microbiol* **64**, 4035-4039.

Figure Legend

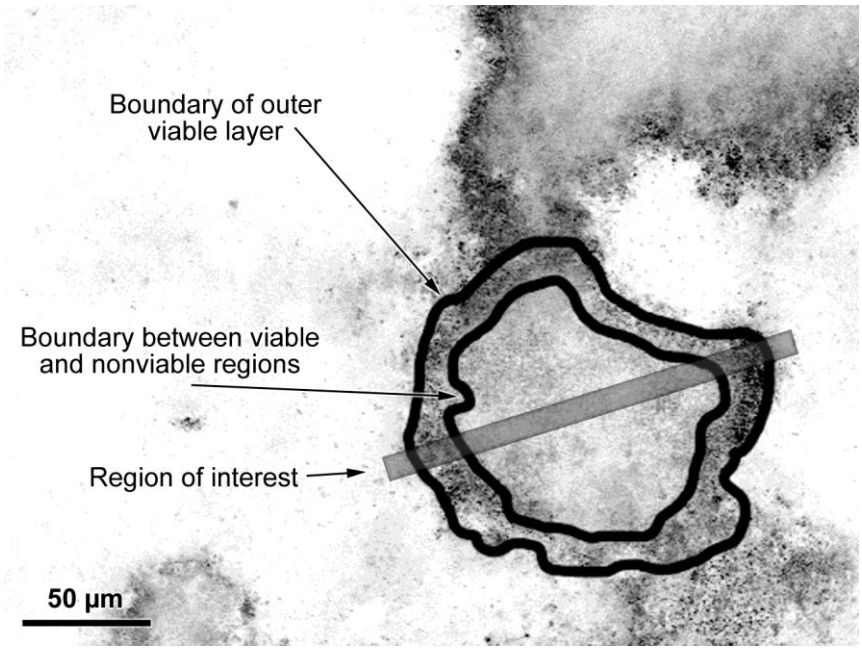

Figure 1 A confocal micrograph of oral biofilm. The region of interest was used to construct the plot-profile shown in figure 2.

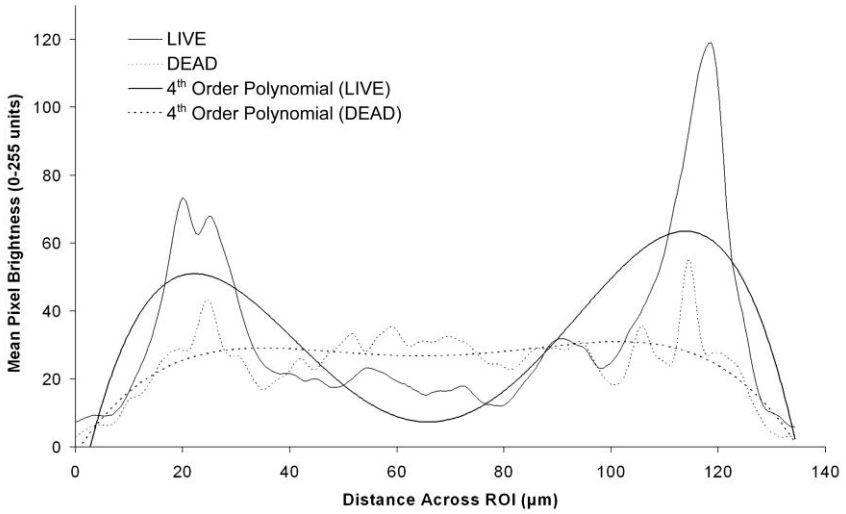

Figure 2 Plot profile across the ROI shown in figure 1.

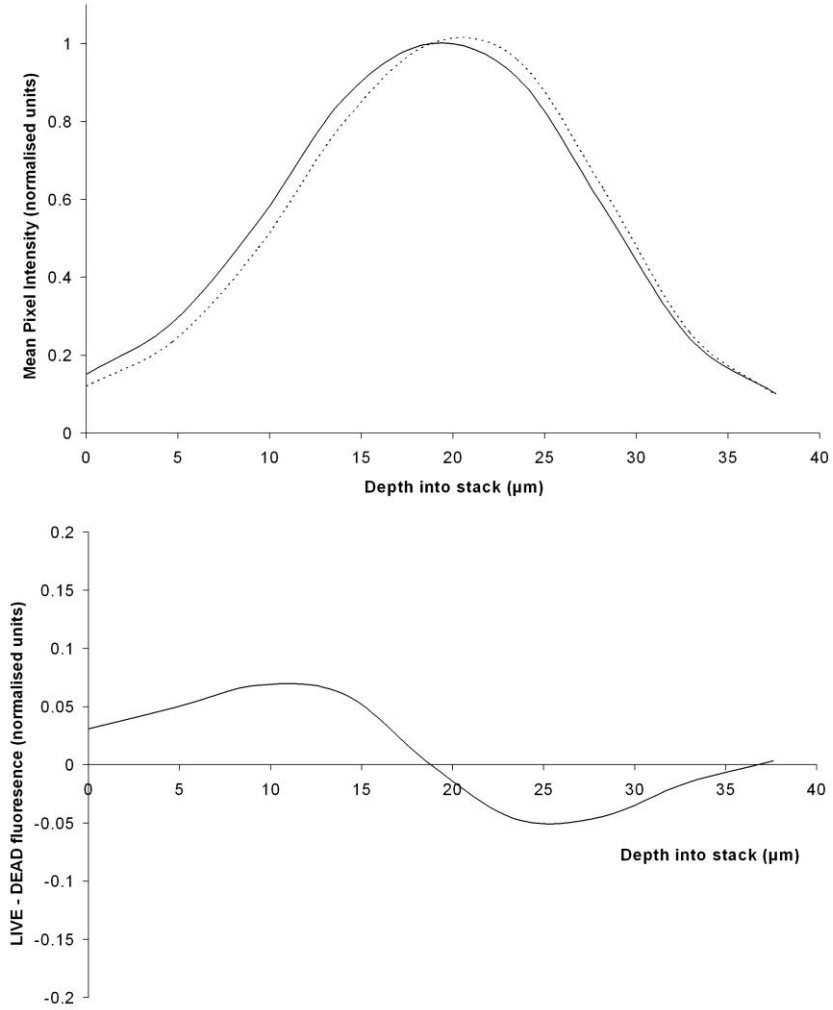

Figure 3a Viability profiles through an oral biofilm.

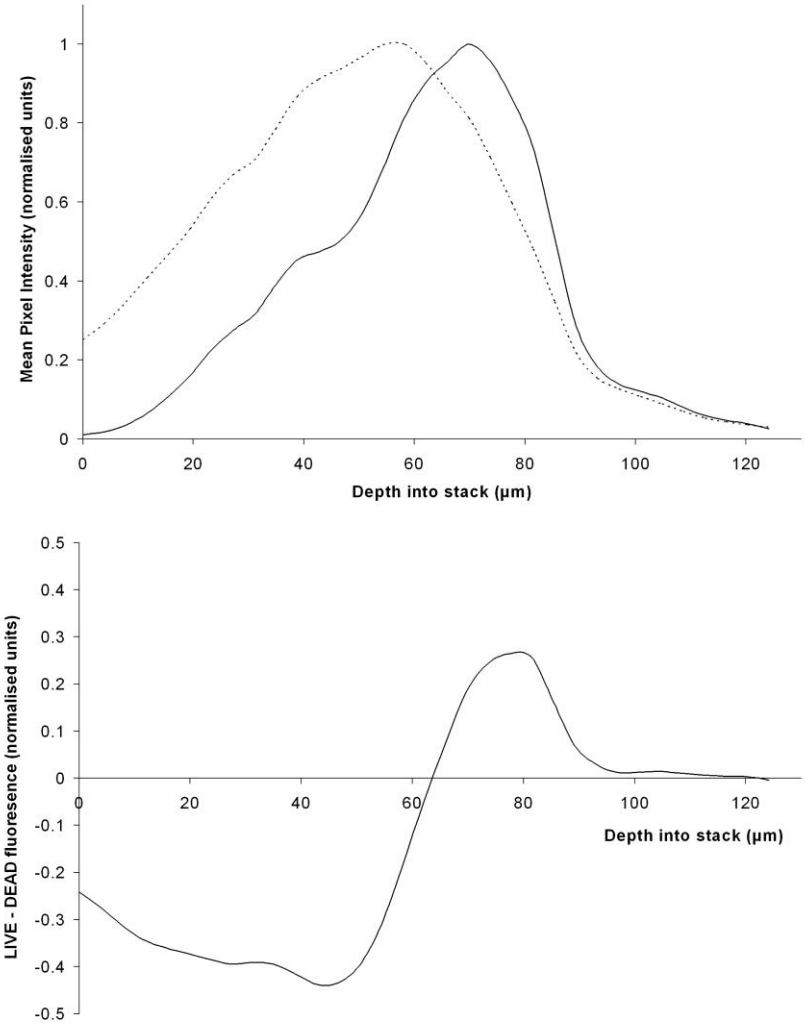
Mean Pixel Intensity (normalised units)
1
0.8
0.6
0.4
0.2
0
0
20
40
60
80
100
120
Depth into stack (µm)
LIVE - DEAD fluoresence (normalised units)
0.5
0.4
0.3
0.2
0.1
0
-0.1
-0.2
-0.3
-0.4
-0.5
0
20
40
60
80
100
120
Depth into stack (µm)

Figure 3b

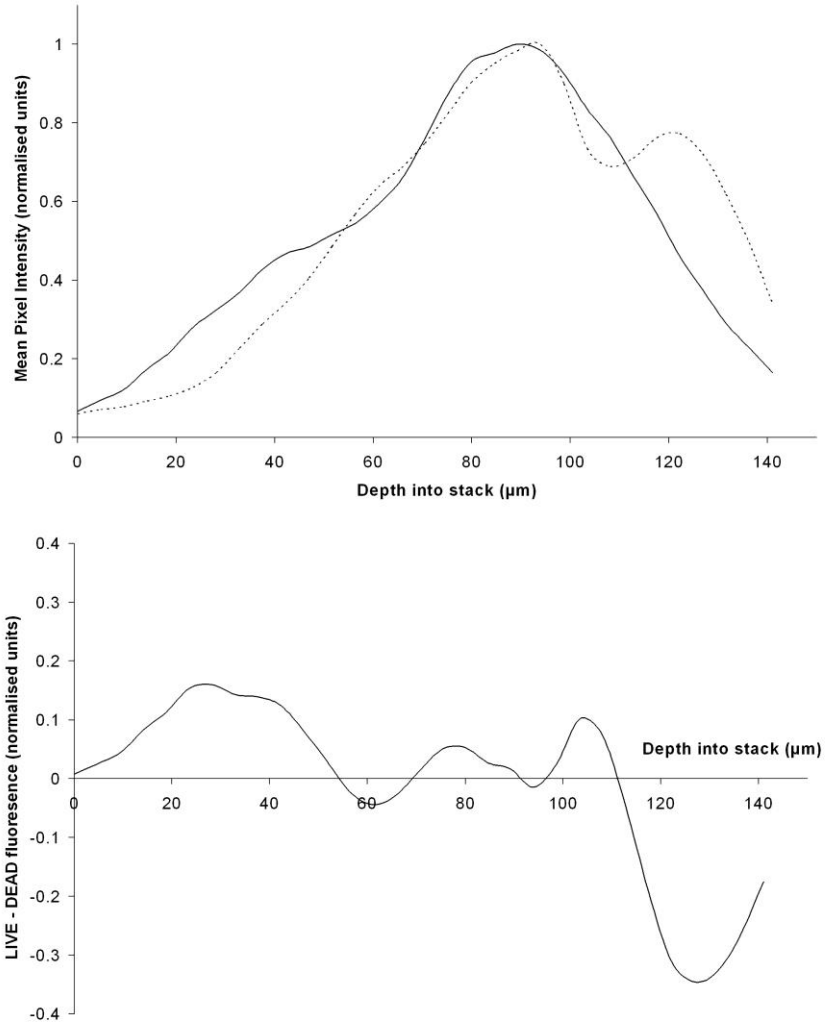
Mean Pixel Intensity (normalised units)
1
0.8
0.6
0.4
0.2
0
0
20
40
60
80
100
120
140
Depth into stack (µm)
LIVE - DEAD fluoresence (normalised units)
0.4
0.3
0.2
0.1
0
-0.1
-0.2
-0.3
-0.4
Depth into stack (µm)

Figure 3c

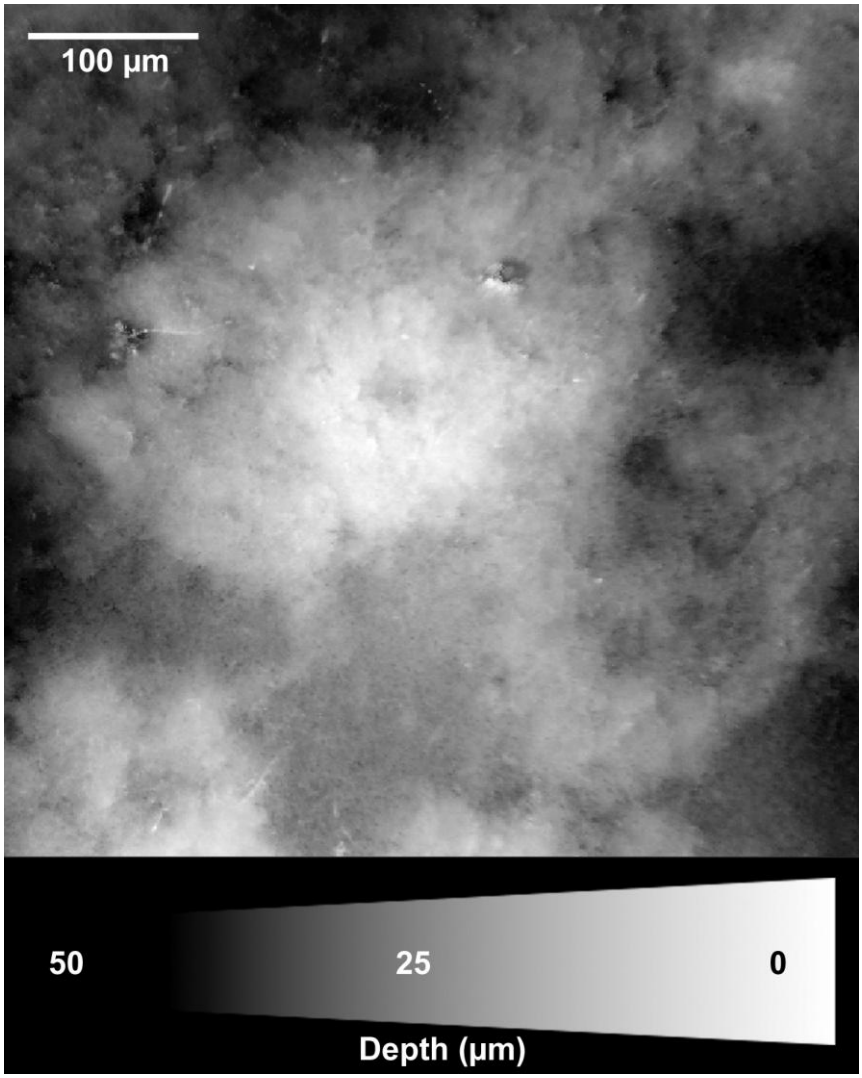

Figure 4 Surface topograph of an oral biofilm.

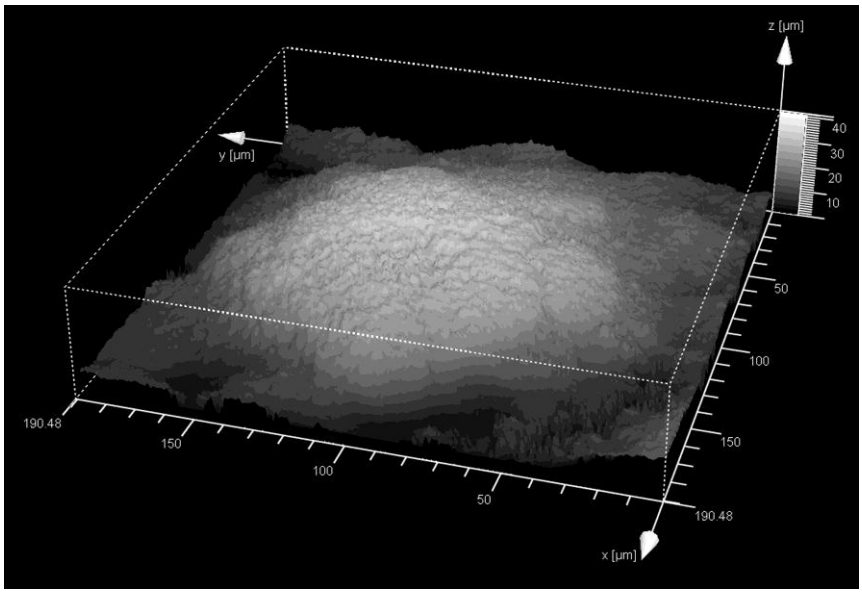

Figure 5 Surface rendering constructed from topographical data (figure 4).

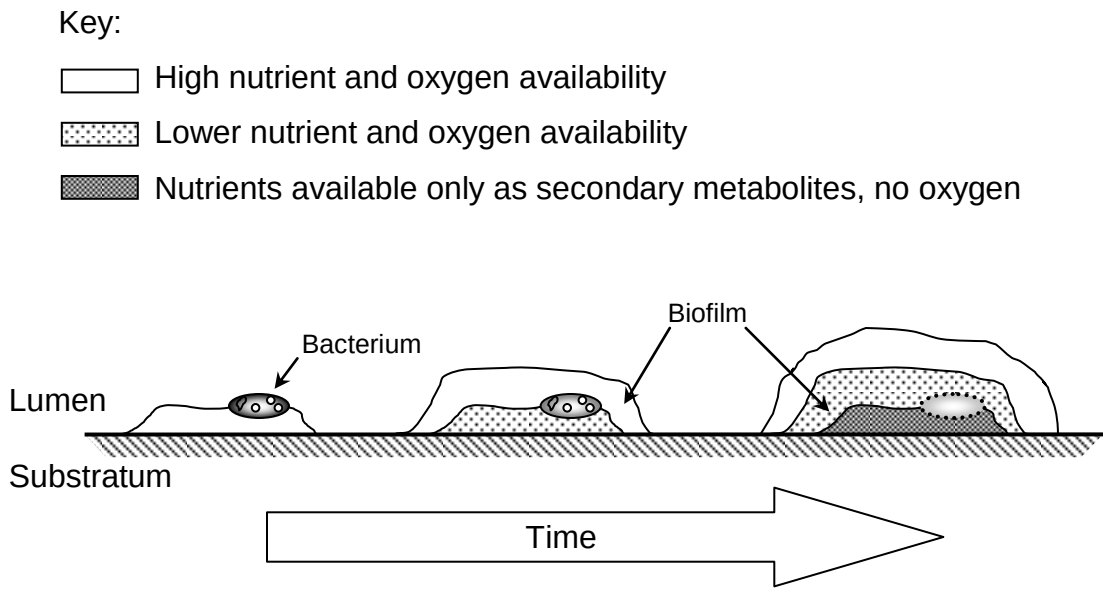

Figure 6 Temporal dislocation of an early colonising bacterium in an oral biofilm